Appl. Phys. B 72, 653–659 (2001) / Digital Object Identifier (DOI) 10.1007/s003400100593

**Applied Physics B**
Lasers
and Optics

# The role of carrier mobility in holographic recording in $LiNbO_3$

**A. Adibi**[1], **K. Buse**[2,*], **D. Psaltis**[3]

[1] Georgia Institute of Technology, School of Electrical and Computer Engineering, Atlanta, Ga. 30332, USA
[2] Universität Bonn, Physikalisches Institut, Wegelerstr. 8, 53115 Bonn, Germany
[3] California Institute of Technology, Department of Electrical Engineering, Pasadena, Calif. 91125, USA

Received: 22 February 2001/Revised version: 5 March 2001/Published online: 27 April 2001 – 

**Abstract.** We investigate the role of carrier mobility in holographic recording in $LiNbO_3$ crystals. Both normal holographic recording (single wavelength, single trap) and two-center recording are considered, and the differences between the performances of the two methods are explained. We show that increasing mobility by using stoichiometric crystals or by doping with Mg does not improve sensitivity considerably, but does reduce $M/\#$ by at least one order of magnitude.

**PACS:** 42.40.-i; 42.40.Pa; 42.40.Ht

Volume holographic storage systems are tried and tested with photorefractive crystals as the recording medium [1]. In such systems, the inhomogeneous illumination created by the interference of the reference and signal beams excites charge carriers from impurity levels into the conduction or valence bands, the charge carriers migrate and they are trapped by empty impurities elsewhere. A space-charge field builds up and modulates the refractive index via the electro-optic effect.

The important material properties are sensitivity ($S$), dynamic range ($M/\#$) and persistence (or non-destructive readout). For several years, lack of persistence was the major drawback of holographic storage in photorefractive crystals, and several methods (thermal fixing [2], electrical fixing [3], two-photon recording [4], frequency-difference holograms [5] and readout with wavevector spectra [6]) were proposed to solve this problem. More recently, two-center holographic recording was proposed and demonstrated [7, 8]. Two-center recording makes storage of persistent holograms possible without sacrificing the dynamic range and sensitivity considerably [9]. The sensitivity of the widely used congruently melting $LiNbO_3$ crystals, however, is still not very good. Therefore, the main challenge in holographic storage in $LiNbO_3$ crystals is the improvement of the sensitivity.

Sensitivity is a measure of recording speed. It is defined as the initial recording slope of the square root of the diffraction efficiency normalized to recording intensity and material thickness. Recording and erasure time constants in holographic recording are approximately inversely proportional to the mobility of the carriers responsible for recording (i.e., electrons in the conduction band or holes in the valence band). Holograms can be recorded faster if we increase the mobility of carriers responsible for recording. Therefore, one idea for increasing sensitivity could be to increase the carrier mobility. In almost all holographic recording experiments in $LiNbO_3$, these carriers are electrons in the conduction band. It is suggested that the mobility of these electrons ($\mu$) can be varied by changing the stoichiometry of $LiNbO_3$: congruently melting $LiNbO_3$ crystals (typical ratio of Li to Nb about 94%) have a lower electron mobility than perfectly stoichiometric crystals (ratio of Li to Nb equal to 1). It is also suggested that the mobility of electrons in the conduction band of $LiNbO_3$ can be varied by highly doping the crystal with magnesium (Mg). Typical doping levels required are of the order of 4 wt. % of MgO [10].

In this paper, we investigate the possibility of increasing the sensitivity in $LiNbO_3$ by increasing the electron mobility. Our assumption is that other material properties (absorption cross-section, recombination coefficient for the different traps, etc.) are fixed, and we only change the mobility of electrons in the conduction band. Two forms of mobility, i.e., drift mobility and Hall mobility, can be defined for ionic crystals (such as $LiNbO_3$) [11]. Throughout this paper, we only use drift mobility. We first consider normal recording with a single wavelength in a typical $LiNbO_3$:Fe crystal. Then, we discuss the role of electron mobility in two-center holographic recording and compare it with that in normal recording.

It is necessary to clarify one important fact here. It is known that the photoconductivity ($\sigma$) of a $LiNbO_3$ crystal can be increased by increasing the stoichiometry [12] or by doping the crystal with so-called damage-resistant impurities

*Corresponding author.
(Fax: +1-404/894-4641, E-mail: adibi@ece.gatech.edu)

(e.g. Mg or Zn) [13]. Increasing photoconductivity results in decreasing recording and erasure time constants of a hologram. Photoconductivity ($\sigma$) varies as

$$\sigma = e\mu n_0 \propto \frac{\mu}{\gamma}\,, \tag{1}$$

where $e$, $\mu$, $n_0$ and $\gamma$ are the electronic charge, electron mobility, average (DC) electron concentration in the conduction band and effective trap recombination coefficient for the electrons in the conduction band, respectively. It has been suggested that the increase in the photoconductivity of stoichiometric or Mg-doped $LiNbO_3$ crystals is due to the increase in the carrier mobility $\mu$. Although this explains all experimental data, it is also possible that the increase in photoconductivity can be due to a reduction in the effective recombination coefficient ($\gamma$). In this paper, we mainly use the first suggestion (i.e., increasing $\mu$ by moving to more stoichiometric crystals or by increasing Mg concentration). However, the results are still valid if the second suggestion is true, because all holographic recording parameters vary with $\mu/\gamma$ instead of varying with $\mu$ or $\gamma$ independently. Therefore, variations of the holographic recording parameters with $\mu$ (while all other parameters including $\gamma$ are fixed) is the same as the variations of the same holographic recording parameters with $1/\gamma$ (while all other parameters including $\mu$ are fixed).

As mentioned above, we assume that changing the stoichiometry of a $LiNbO_3$ crystal or doping it with Mg changes only the photoconductivity considerably. In our analysis, we assume that other crystal parameters, especially the bulk photovoltaic constant and the absorption cross-section of the Fe traps, are not modified considerably by changing the stoichiometry of the crystal or by doping it with Mg. Our justification for this assumption is the work by Sommerfeldt et al. [13], in which different parameters of $LiNbO_3$:Fe crystals with different degrees of stoichiometry or different Mg concentrations were measured. Sommerfeldt et al. showed that photoconductivity is the only parameter that varies considerably by changing the stoichiometry or by doping with Mg.

## 1 Effect of carrier mobility in normal holographic recording

To study the effect of $\mu$ on $M/\#$ [14] and $S$, we consider the dependence of the saturation hologram strength ($A_0$) and recording time constant ($\tau_r$) on $\mu$. We assume that recording and erasure time constants are approximately the same, resulting in

$$M/\# = \frac{A_0\tau_e}{\tau_r} \simeq A_0\,, \tag{2}$$

where $\tau_e$ is the erasure time constant. Note that even if $\tau_r$ and $\tau_e$ are not the same, they have similar variations with $\mu$. Therefore, the main parameter that represents the effect of $\mu$ on $M/\#$ is $A_0$. Note also that $A_0$ is linearly proportional to the saturation space-charge field $E_{1,sat}$. Therefore, we can use

$$M/\# \propto A_0 \propto E_{1,sat} \tag{3}$$

to study the effect of $\mu$ on $M/\#$.

The effect of $\mu$ on $S$ can be studied by using

$$S = \frac{A_0/\tau_r}{I_R L} \propto \frac{E_{1,sat}}{\tau_r}\,, \tag{4}$$

where $I_R$ and $L$ represent recording intensity and crystal thickness, respectively. $I_R$ and $L$ are independent of $\mu$.

The approximate formulas for $E_{1,sat}$ and $\tau_r$ are

$$E_{1,sat} = -\frac{j_{phv1} + j_{diff1}}{e\mu n_0}\,, \tag{5}$$

$$\tau_r = \frac{\varepsilon\varepsilon_0}{e\mu n_0}\,, \tag{6}$$

where $e$ and $n_0$ are the electronic charge and the spatially averaged (DC) electron concentration in the conduction band, respectively. Here, $\varepsilon$ and $\varepsilon_0$ are the dielectric constant (or relative permittivity) of the recording material and the permittivity of free space, respectively. Furthermore, $j_{phv1}$ and $j_{diff1}$ are the first Fourier components of the bulk photovoltaic and diffusion current densities, respectively. Furthermore, $n_0$ can be approximately represented by

$$n_0 \simeq \frac{q_{Fe}s_{Fe}N_{Fe0}^{-}I_{R0}}{\gamma_{Fe}(N_{Fe} - N_{Fe0}^{-})}\,, \tag{7}$$

where $q_{Fe}s_{Fe}$ and $\gamma_{Fe}$ represent the absorption cross-section for excitation of electrons from Fe traps to the conduction band and the recombination coefficient of the Fe traps, respectively. Furthermore, $N_{Fe}$, $N_{Fe0}^{-}$, and $I_{R0}$ represent total Fe concentration, DC electron concentration in the Fe traps and DC recording intensity, respectively. The formulas for $j_{phv1}$ and $j_{diff1}$ in $LiNbO_3$:Fe are

$$j_{phv1} \simeq \kappa_{Fe}N_{Fe0}^{-}I_{R1} \tag{8}$$

$$j_{diff1} = k_B T\mu\nabla n_1 = \mathrm{i}Kk_B T\mu n_1\,. \tag{9}$$

$\kappa_{Fe}$ and $I_{R1}$ in (8) are the bulk photovoltaic constant of the Fe traps at the recording wavelength and the amplitude of sinusoidal recording intensity, respectively. In (9) $k_B$, $T$, $K$, and $n_1$ represent the Boltzmann constant, the absolute temperature, the amplitude of the grating vector of the hologram and the first Fourier component of the electron concentration in the conduction band. For holographic recording in congruently melting $LiNbO_3$:Fe crystals using transmission geometry, the bulk photovoltaic current is dominant and the diffusion current density ($j_{diff1}$) in (5) can be neglected, resulting in

$$E_{1,sat} \simeq -\frac{j_{phv1}}{e\mu n_0} \simeq -\frac{\kappa_{Fe}N_{Fe0}^{-}I_{R1}}{e\mu n_0}\,. \tag{10}$$

Replacing $n_0$ in (10) by its equivalent from (7), we obtain

$$|E_{1,sat}| \simeq \frac{\kappa_{Fe}\gamma_{Fe}(N_{Fe} - N_{Fe0}^{-})I_{R1}}{eq_{Fe}s_{Fe}I_{R0}}\frac{1}{\mu} \propto \frac{1}{\mu}\,. \tag{11}$$

Putting (6) and (11) into (3) and (4), we obtain the dependence of $M/\#$ and $S$ on $\mu$ as

$$M/\# \propto \frac{1}{\mu}\,, \tag{12}$$

$$S = C\,, \tag{13}$$

where $C$ represents some constant independent of $\mu$. Note that (12) and (13) are valid only in the regime where there is a domination of the bulk photovoltaic current. Therefore, these equations can be typically applied to congruently melting crystals in transmission geometry. Equations (12) and (13) suggest that we cannot increase the sensitivity by increasing $\mu$, while we lose $M/\#$. This result might seem strange at first, since we know that the holograms are recorded faster at higher $\mu$ (recording time constant becomes smaller at higher $\mu$). However, sensitivity depends on the ratio of saturation hologram strength ($A_0$) and recording time constant ($\tau_r$). When the bulk photovoltaic current is dominant, both $A_0$ and $\tau_r$ decrease with increasing $\mu$ in a similar way, resulting in the approximate independence of sensitivity of $\mu$.

The situation is completely different in the regime where the diffusion current is dominant. This is the case for stoichiometric $LiNbO_3$:Fe crystals, or in some cases, for congruently melting crystals in the 90° or reflection geometries. The saturation space-charge field in this regime can be represented by

$$E_{1,\mathrm{sat}} = -\frac{j_{\mathrm{diff}1}}{e\mu n_0} \simeq -\mathrm{i}K\frac{k_\mathrm{B}T}{e}\frac{n_1}{n_0}\,. \tag{14}$$

Assuming unity modulation depth of recording intensity, we can use $n_1 \simeq n_0$ to simplify (14) to

$$|E_{1,\mathrm{sat}}| \simeq \frac{k_\mathrm{B}T}{e}K\,. \tag{15}$$

Equation (15) suggests that in the regime where the diffusion current dominates the saturation space-charge field is approximately independent of $\mu$. Using this result, we can summarize the dependence of $M/\#$ and $S$ on $\mu$ in this regime as

$$M/\# = C' \tag{16}$$

$$S \propto \mu\,, \tag{17}$$

where $C'$ is a constant independent of $\mu$. Equations (16) and (17) suggest that increasing mobility in the regime where the diffusion current dominates is a good idea for increasing sensitivity without affecting $M/\#$. In this regime, the saturation hologram strength is independent of $\mu$. Therefore, increasing $\mu$ results in increasing sensitivity by reducing the recording time constant. The diffusion current dominates in $LiNbO_3$ in near–stoichiometric crystals or in crystals that are highly doped with MgO, or in some cases in the 90° or reflection geometries with small grating period (or high spatial frequency).

As discussed above, we need to get to the regime where the diffusion current dominates in $LiNbO_3$:Fe to start improving sensitivity by increasing $\mu$. To do this, we need to increase $\mu$ by using stoichiometric crystals, for example. However, we lose $M/\#$ by a large factor in going from the regime where the photovoltaic current dominates to that where the diffusion current dominates. This is clearly depicted in Fig. 1, which shows the theoretical variation of the saturation hologram strength ($A_0 \simeq M/\#$) and $S$ with $\mu$ in a 0.85-mm-thick $LiNbO_3$ crystal doped with 0.075 wt. % $Fe_2O_3$. The calculation is performed by solving the band-transport equations [15] numerically using Fourier development. We assumed that recording was performed by two red beams (wavelength 633 nm, intensity of each beam 250 mW/cm$^2$).

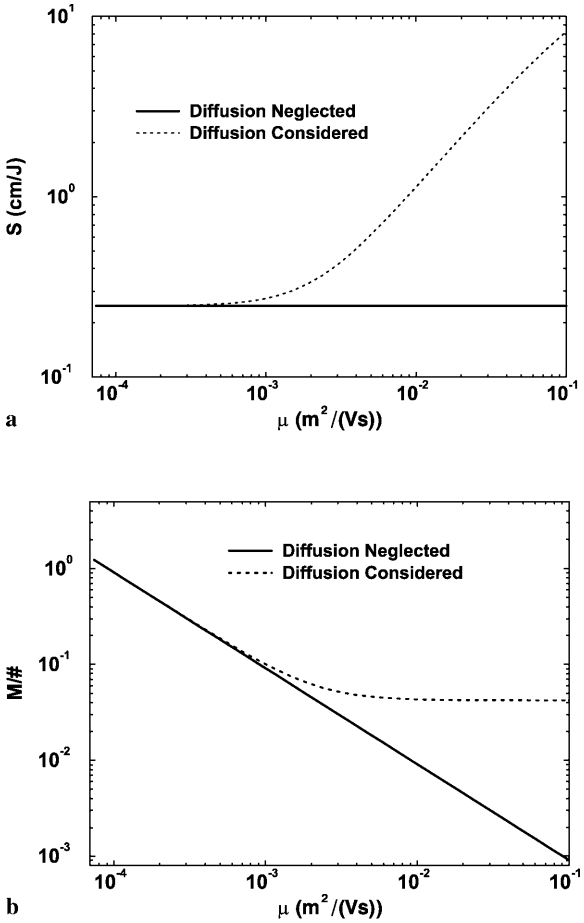


**Fig. 1a,b.** Theoretical variations of **a** sensitivity ($S$) and **b** approximate dynamic range ($M/\#$) with electron mobility ($\mu$) for a 0.85-mm-thick $LiNbO_3$:Fe crystal in normal recording. It is assumed that the crystal is doped with 0.075 wt. % $Fe_2O_3$ and 13.5% of the Fe traps are initially occupied with electrons ($N_{\mathrm{Fe}} = 2.5\times10^{25}$ m$^{-3}$ and $N_{\mathrm{Fe}}^{-} = 3.4\times10^{24}$ m$^{-3}$). It is also assumed that recording is performed by two red beams (wavelength 633 nm, intensity of each beam 250 mW/cm$^2$, ordinary polarization, angle between each beam and the normal to the surface outside the crystal 20°)

Although 633 nm is not the best wavelength for recording from Fe traps, we chose it to be the same as the recording wavelength in the two-center recording discussed later. The two curves in each part of Fig. 1 are calculated with and without considering the diffusion current to show the regimes where the different components of current dominate. As Fig. 1 shows, we need to increase $\mu$ by more than one order of magnitude from that of a typical congruently melting $LiNbO_3$ crystal to enter into the regime where the diffusion current dominates, where sensitivity can be improved by increasing $\mu$ further. During this process, $M/\#$ is reduced by more than one order of magnitude before getting to the regime where the diffusion current dominates, where $M/\#$ becomes almost independent of $\mu$. It is important to note that the range of $\mu$ shown in Fig. 1 is not the practical range that can be obtained by changing the stoichiometry of $LiNbO_3$ crystals. It is not practically possible to increase $\mu$ in $LiNbO_3$ by three orders of magnitude by simply changing the stoichiometry of the crystal or by doping it with MgO. Therefore, the usage of stoichiometric crystals or of crystals doped highly with MgO in the transmission geometry is not a good idea to

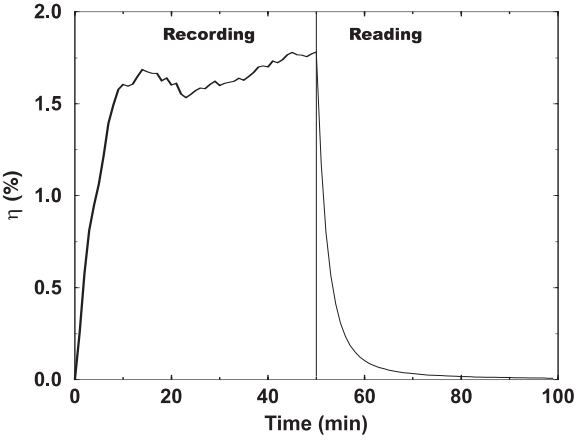


**Fig. 2.** Recording and read-out curve for a plane wave hologram in a 0.85-mm-thick $LiNbO_3$:Fe:Mg crystal. Recording is performed by two coherent beams (wavelength 488 nm, intensity of each beam 15.5 mW/cm$^2$, ordinary polarization). Read-out is performed by one of the recording beams

improve $S$. While $S$ of these materials is similar to that of congruently melting crystals, their $M/\#$ is much smaller than that of the congruently melting crystals.

Figure 2 shows the recording and read-out curve for a plane-wave hologram recorded in a 0.85-mm-thick $LiNbO_3$ crystal doped with 0.025 wt. % $Fe_2O_3$ and 4.3 wt. % MgO. Recording is performed in transmission geometry by two plane waves (wavelength 488 nm, intensity of each beam 15.5 mW/cm$^2$, ordinary polarization) while reading is performed by one of the recording beams. The values of $M/\#$ and $S$ calculated from Fig. 2 are $M/\# = 0.15$ and $S = 0.15$ cm/J. Although $S = 0.15$ cm/J is of the same order of sensitivity that can be obtained in congruently melting $LiNbO_3$:Fe crystals, the value of $M/\#$ is much lower than those obtained in congruent $LiNbO_3$:Fe crystals with similar properties.

## 2 Effect of carrier mobility in two-center holographic recording

One might expect that similar behaviors of $M/\#$ and $S$ with carrier mobility are obtained in two-center recording, since alteration of the mobility would affect electron transport in the conduction band in a similar way for both normal and two-center recording. However, the effect of mobility on $M/\#$ and $S$ in two-center recording is very different from that in normal recording. Figure 3 shows the theoretical variation of $S$ and final saturation hologram strength (approximately equivalent to $M/\#$) with $\mu$ in two-center holographic recording in a $LiNbO_3$ crystal doped with 0.075 wt. % $Fe_2O_3$ and 0.01 wt. % MnO. In this calculation we assumed that all Fe traps as well as 10% of the Mn traps are initially empty. We also assumed that recording was performed by one homogeneous UV beam (wavelength 365 nm, intensity 20 mW/cm$^2$) and two interfering red beams (wavelength 633 nm, intensity of each beam 250 mW/cm$^2$). The two curves in each part of Fig. 3 are calculated with and without considering diffusion currents to show the regimes where the diffusion and bulk photovoltaic currents dominate. The calculations for Fig. 3 are performed using the two-center model described

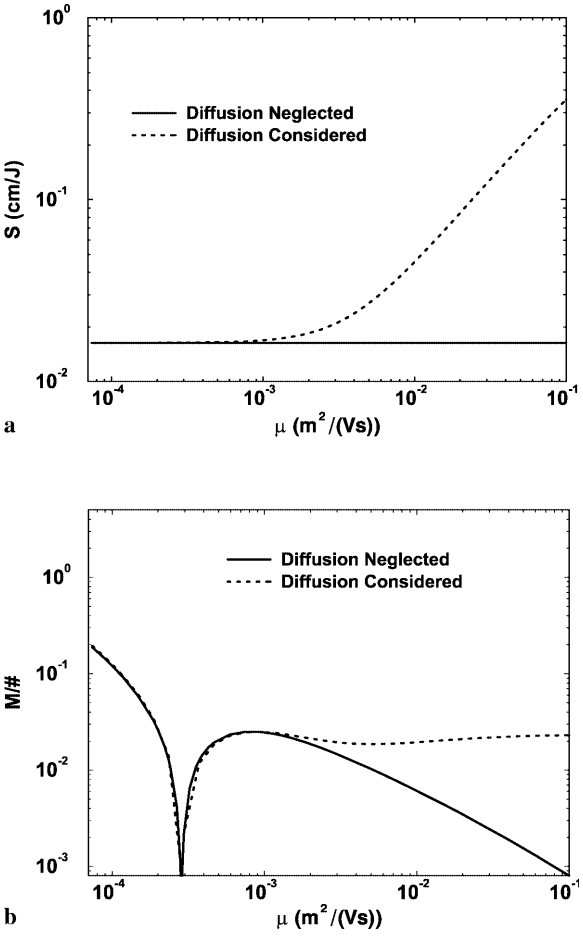


**Fig. 3a,b.** Theoretical variations of **a** sensitivity ($S$) and **b** approximate $M/\#$ with electron mobility ($\mu$) for a 0.85-mm-thick $LiNbO_3$:Fe:Mn crystal in two-center recording. It is assumed that the crystal is doped with 0.075 wt. % $Fe_2O_3$ and 0.01 wt. % MnO. All Fe traps as well as 10% of the Mn traps are initially empty ($N_{Fe} = 2.5 \times 10^{25}$ m$^{-3}$, $N_{Fe}^{-} = 0$, $N_{Mn} = 3.8 \times 10^{24}$ m$^{-3}$ and $N_{Mn}^{-} = 3.4 \times 10^{24}$ m$^{-3}$). It is assumed that recording is performed by one UV beam (wavelength 365 nm, intensity 20 mW/cm$^2$) and two red beams (wavelength 633 nm, intensity of each beam 250 mW/cm$^2$, ordinary polarization)

in [8]. As Fig. 3a shows, the variation of sensitivity ($S$) in two-center recording is similar to that in normal recording (Fig. 1a). However, the variation of the persistent $M/\#$ with $\mu$ in two-center recording is totally different from that in normal recording, as Fig. 3b shows. The $M/\#$ in two-center recording decreases initially with increasing $\mu$, going to zero at one value of $\mu$. It then increases with further increasing $\mu$ and finally becomes constant in the diffusion-dominated regime.

To understand the unexpected variation of persistent $M/\#$ with $\mu$, we use the energy band diagram for a $LiNbO_3$:Fe:Mn crystal shown in Fig. 4. During recording, electrons are excited from the Fe traps to the conduction band by recording light. An electron moves a short distance before being trapped by $Fe^{3+}$ centers. An electron on average goes through several of these cycles of excitation to the conduction band, moving in the conduction band and becoming trapped. The presence of the sensitizing (UV) beam also brings the electrons that fall into the Mn traps back to the Fe traps during recording. During read-out, the sensitizing beam is blocked. Therefore, electrons are excited to the conduction band primarily from the Fe traps. Electrons that fall into Mn traps cannot be excited back

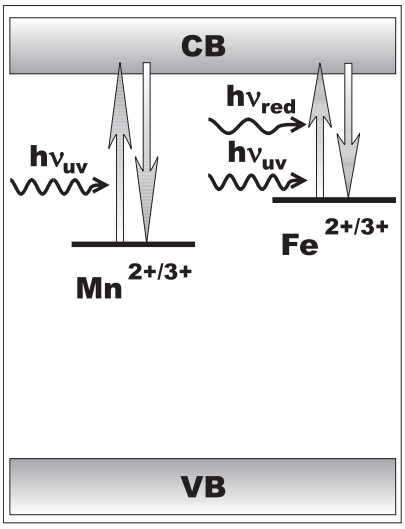


**Fig. 4.** Energy band diagram of a $LiNbO_3$:Fe:Mn crystal

to the conduction band by the read-out light. During read-out on average an electron in the Fe traps will end up in Mn traps after only a few cycles of excitation to the conduction band. This asymmetry between the average number of excitations, movements and trapping cycles for an electron during recording and read-out is the main reason for the persistence obtained in two-center recording. At low values of $\mu$, an electron on average goes through many of these cycles to record a strong hologram, while at read-out it only goes through at most a few cycles before being trapped at Mn centers. Therefore, we only see a small partial erasure of the hologram during read-out at low values of $\mu$, and we observe relatively high persistent $M/\#$ at low $\mu$. The asymmetry between the number of cycles during recording and read-out is reduced as $\mu$ increases, since the average distance an electron moves in the conduction band in each cycle is linearly proportional to $\mu$. Therefore, the average number of cycles an electron undergoes during recording decreases with increasing $\mu$. On the other hand, the average number of cycles an electron undergoes during read-out does not strongly depend on $\mu$ as it is mainly determined by the relative probabilities for electron trapping at Fe and Mn centers. Therefore, the average distance an electron moves backward during read-out becomes closer to the average distance an electron moves forward during recording as $\mu$ increases. This results in a stronger partial erasure and smaller persistent $M/\#$ at higher values of $\mu$. The lowest persistent $M/\#$ is obtained at the specific value of $\mu$ that results in the total disappearance of the asymmetry during recording and read-out. For this specific value of $\mu$, the hologram is completely erased during read-out, resulting in zero persistent $M/\#$. If we increase $\mu$ further, we expect the hologram to undergo a 180° phase shift during read-out. In other words, the electron transfer from Fe traps to Mn traps during read-out causes the diffraction efficiency to go first to zero at some time. At this time, the two holograms in Fe traps and Mn traps are equally strong, but they are exactly 180° out of phase. Therefore, the total hologram strength (sum of the two holograms) is zero. The remaining space-charge pattern (or electron concentration) in the Fe traps will be transferred to the Mn traps via the conduction band during further read-out. However, these electrons move in the conduction band, and this movement results in a nonzero hologram strength. The phase difference between this newly revealed hologram and the original one is 180°. As $\mu$ increases from its specific value (resulting in zero persistent $M/\#$), the revealed hologram during read-out becomes stronger, and $M/\#$ increases with increasing $\mu$, as shown in Fig. 3b. Figure 5 shows theoretical recording and read-out curves for plane-wave holograms recorded in the $LiNbO_3$:Fe:Mn crystal discussed before at different values of $\mu$. The 180° phase shift obtained during read-out at very high $\mu$ as well as the total erasure of the hologram during read-out at a specific value of $\mu$ are evident from Fig. 5.

It is important to note that the sensitivity values shown in Fig. 3a were calculated without considering persistence. If we are interested in the persistent sensitivity, we need to modify this value by the partial erasure of the hologram during read-out, as explained in [9]. This results in even lower values of sensitivity, especially around the specific value of $\mu$ that gives zero $M/\#$.

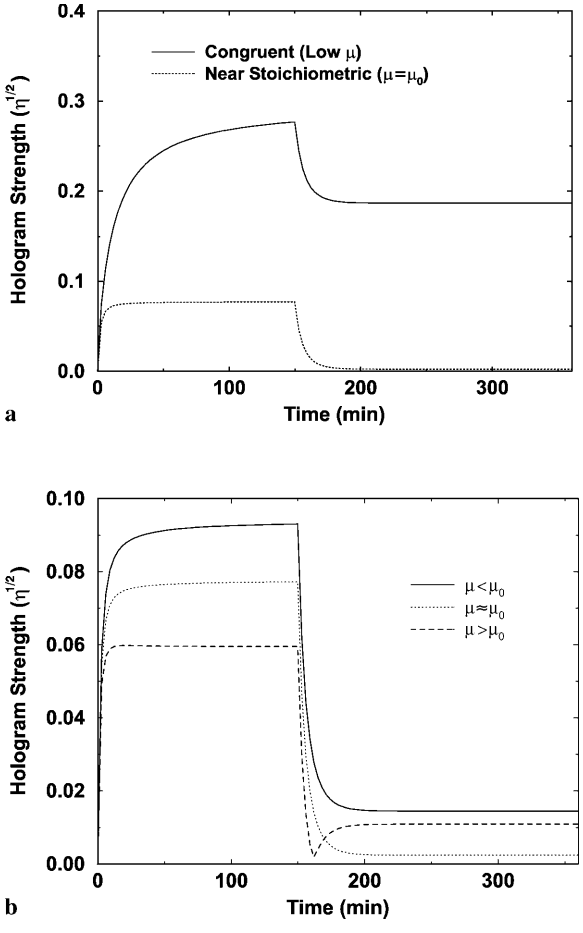


**Fig. 5a,b.** Theoretical recording and read-out curves for a 0.85-mm-thick $LiNbO_3$:Fe:Mn crystal in two-center recording. The curves were calculated using different values of electron mobility ($\mu$). The crystal parameters used in these calculations are the same as those given in the caption of Fig. 3. It is assumed that recording is performed by one UV beam (wavelength 365 nm, intensity 20 mW/cm$^2$) and two red beams (wavelength 633 nm, intensity of each beam 250 mW/cm$^2$, ordinary polarization). **a** Comparison of recording and read-out curves of a congruent (low $\mu$) crystal with that of a crystal with a special value of $\mu$ ($\mu_0$), resulting in zero final $M/\#$. **b** Comparison of the recording and read-out curves for different values of $\mu$ in the vicinity of $\mu = \mu_0$

To investigate the possibility of sensitivity improvement in two-center recording by increasing the electron mobility, we performed experiments with a 5-mm-thick $LiNbO_3$ crystal doped with 0.075 wt. % $Fe_2O_3$, 0.01 wt. % MnO, and 4.3 wt. % MgO. The oxidation of the crystal to the level where all Fe traps as well as a portion of the Mn traps are empty (as required for two-center recording) was very difficult. This difficulty is a typical property of the Mg doped or stoichiometric $LiNbO_3$ crystals, making the optimization of annealing in two-center recording complex or even impossible. The physical reason is that more stoichiometric or Mg-doped crystals have less defects that allow charge compensation upon thermal annealing. Although we oxidized the crystal for three consecutive days at 1000–1100 °C in an $O_2$ atmosphere, there was still a small electron concentration in the Fe traps, and all Mn traps were occupied by electrons. We recorded a plane-wave hologram using one homogeneous sensitizing beam (wavelength 404 nm, intensity 3.6 mW/cm$^2$) and two recording beams (wavelength 514 nm, intensity of each beam 17 mW/cm$^2$, ordinary polarization) in transmission geometry. To have a recording curve that is appropriate for measuring sensitivity, we first recorded a hologram after pre-exposing the crystal to the sensitizing beam for 2 h. Then, we rotated the crystal until the read-out of the hologram was negligible. This preparation assures that a steady-state balance between sensitization and bleaching is already achieved; the electron concentrations in the Mn and Fe traps are now very close to the steady-state values that are obtained during recording. After this careful adjustment of the starting condition, we recorded a hologram in the new location while monitoring its diffraction efficiency with time. Read-out of the hologram was then performed by one of the recording beams. The experimental recording and read-out curve is shown in Fig. 6. The value of sensitivity from Fig. 6 is $S = 0.05\,\mathrm{cm/J}$, which is not better than that obtained with a congruently melting $LiNbO_3$ crystal with similar Fe and Mn concentrations. Note that the crystal used in this experiment was too reduced for persistent two-center holographic recording. As mentioned above, we were not able to oxidize the crystal enough to leave all Fe traps empty. However, the sensitivity is defined by recording mechanisms, and having a small electron concentration in the Fe traps only increases the sensitivity. The sensitization mechanism during recording brings several electrons from the Mn traps to the Fe traps, as it does in two-center recording. The excessive reduction (extra electron concentration in the Fe traps) results in the higher value of sensitivity than that obtained in a crystal with the correct oxidation/reduction state. Therefore, we would expect that persistent sensitivity in the $LiNbO_3$:Fe:Mn:Mg crystal is even less than $S = 0.05\,\mathrm{cm/J}$, which is not better than that in the congruently melting $LiNbO_3$:Fe:Mn crystal.

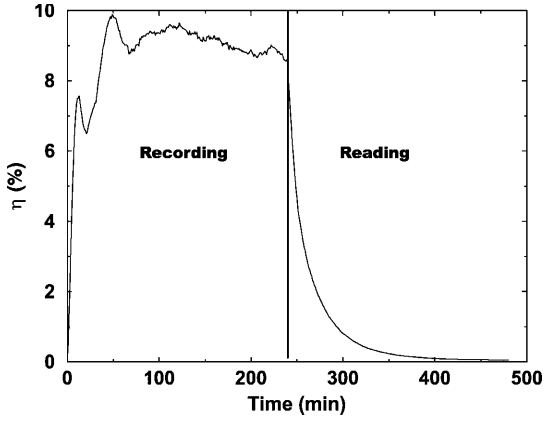


**Fig. 6.** Recording and read-out curve for a plane wave hologram in a 5-mm-thick $LiNbO_3$:Fe:Mn:Mg crystal. Recording is performed by one sensitizing beam (wavelength 404 nm, intensity 3.6 mW/cm$^2$) and two coherent beams (wavelength 514 nm, intensity of each beam 17 mW/cm$^2$, ordinary polarization). Read-out is performed by one of the recording beams

One important point to address here is the role of stoichiometry in two-step holographic recording. It was shown recently that better $S$ and $M/\#$ can be obtained in two-step recording in undoped stoichiometric $LiNbO_3$ compared to the congruent crystals [16, 17]. One might consider this as a contradiction to the results of this paper. However, the role of stoichiometry in two-step recording is the elongation of the lifetime of electrons in the shallow polaron levels in $LiNbO_3$. Increasing this lifetime increases the sensitization efficiency and reduces the minimum intensity required for holographic storage. Therefore, better $S$ and $M/\#$ are obtained. This improvement is not due to the change in $\mu$. Our results suggest that if the same polaron concentration and polaron lifetime can be obtained with lower $\mu$, we would obtain better $M/\#$ without sacrificing $S$.

## 3 Role of mobility in 90° and reflection geometries

In the previous sections, we primarily concentrated on holographic recording in the transmission geometry, because it offers the maximum $S$ and $M/\#$ [18]. Both $M/\#$ and $S$ depend linearly on the electro-optic coefficient of the recording crystal. For recording with extraordinary polarization in transmission geometry in $LiNbO_3$, the relevant electro-optic coefficient is $r_{33}$, which is the largest electro-optic coefficient of $LiNbO_3$. For recording in 90° and reflection geometries, however, we cannot use extraordinary polarization. Therefore, the relevant electro-optic coefficient is $r_{13}$, which is about three times smaller than $r_{33}$. On the other hand, there are some applications where reflection and 90° geometries might be the better choice.

Besides the possible polarization for the recording beams, the other major difference between the different recording geometries is the strength of the diffusion field. Equation (15) shows that the diffusion field depends linearly on the magnitude of the grating vector ($\boldsymbol{K}$). For recording in symmetric transmission geometry with the angle between each recording beam and the normal to the surface outside the crystal being $\theta$, $K$ is

$$K = \frac{4\pi}{\lambda} \sin\theta\,, \tag{18}$$

while it is $K = 2\sqrt{2}\pi n/\lambda$ and $K = 4\pi n/\lambda$ for 90° and reflection geometries, respectively. In these formulas, $\lambda$ and $n$ are the recording wavelength in free space and the index of refraction for $LiNbO_3$ at the recording wavelength ($n \simeq 2.3$ for visible light), respectively.

Table 1 summarizes the theoretically calculated values of $M/\#$ and $S$ in normal holographic recording with differ-

**Table 1.** Theoretical values of $M/\#$ and $S$ obtained in a 0.85-mm-thick $LiNbO_3$:Fe crystal with normal recording and different recording geometries. It is assumed that the crystal is doped with 0.075 wt. % $Fe_2O_3$ and 13.5% of the Fe traps are initially occupied with electrons. It is also assumed that recording is performed by two red beams (wavelength 633 nm, intensity of each beam 250 $mW/cm^2$). Cong., Stoi., and Mg-doped: congruent, near-stoichiometric, and Mg-doped crystals, respectively. o-pol and e-pol: ordinary polarization and extraordinary light polarization for the recording beams, respectively. In transmission geometry calculations, the angle between each recording beam and the normal to the surface outside the crystal is $\theta = 20°$

| Recording geometry<br>Material | $M/\#$<br>Cong. | $M/\#$<br>Stoi./Mg-doped | $S$ (cm/J)<br>Cong. | $S$ (cm/J)<br>Stoi./Mg-doped |
|---|---|---|---|---|
| Transmission (e-pol) | 3.6 | 0.39 | 0.75 | 0.78 |
| Transmission (o-pol) | 1.2 | 0.13 | 0.25 | 0.26 |
| 90 °C (o-pol) | 1.2 | 0.20 | 0.25 | 0.48 |
| Reflection (o-pol) | 1.2 | 0.29 | 0.25 | 0.62 |

ent recording geometries for a congruent $LiNbO_3$:Fe crystal and a near-stoichiometric one. The crystal properties are the same as those in the caption of Fig. 1. In these calculations, we assumed that $\mu$ in the near-stoichiometric crystal is 10 times larger than that in the congruent crystal ($\mu = 7.4 \times 10^{-5}\,m^2/V\,s$ for the congruent crystal and $\mu = 7.4 \times 10^{-4}\,m^2/V\,s$ for the near-stoichiometric crystal). Furthermore, we assumed the angle between each recording beam and the normal to the surface outside the crystal in transmission geometry to be $\theta = 20°$. Note also that, although both ordinary and extraordinary polarizations can be used in transmission geometry, only ordinary polarization can be used in 90° and reflection geometries.

We can conclude from Table 1 that, if one chooses to use the 90° geometry, using stoichiometric crystals can result in an improvement in $S$ by a factor of about 2, and the price is a reduction in $M/\#$ by a factor of about 6. Using stoichiometric crystals in the reflection geometry results in an improvement in $S$ by a factor of about 2.5 but in a reduction of $M/\#$ by a factor of about 4 compared to a congruent crystal in the same geometry. However, neither 90° geometry nor reflection geometry (even with a stoichiometric crystal) can result in a $S$ better than that obtained using a congruent crystal in transmission geometry with extraordinary polarization. The results of Table 1 suggest that increasing $\mu$ of a $LiNbO_3$ crystal within the practical range (by one order of magnitude) does not improve $S$ (compared to the best value obtained using a congruent crystal) but reduces $M/\#$ by at least one order of magnitude. Although we considered only normal holographic recording in this section, similar results can be obtained for two-center recording.

## 4 Conclusion

We showed that we cannot increase sensitivity ($S$) in either normal or two-center holographic recording in $LiNbO_3$ crystals by increasing electron mobility ($\mu$). The practical $\mu$ that can be obtained by using stoichiometric crystals or by doping the crystal highly with MgO is not high enough to increase $S$ considerably beyond that obtained in congruently melting crystals. On the other hand, we lose dynamic range ($M/\#$) by a large factor by using stoichiometric or Mg doped $LiNbO_3$ crystals in both normal and two-center recording.

The understanding of the effect of $\mu$ on the performance of two-center holographic recording systems discussed here is very important in the investigation of other materials for persistent two-center holographic recording. It is logical to use materials with lower values of $\mu$ to obtain good persistent $M/\#$ in two-center recording. Therefore, in designing a holographic recording system using $LiNbO_3$, we need to use a congruently melting doubly doped crystal. Note that crystals with Li concentrations smaller than that in a congruently melting crystal can be grown too. Such crystals have smaller values of $\mu$ than that of a congruently melting crystal. However, the crystal quality is typically not as good as that of the congruently melting crystals.

Note that, although we used holographic recording experiments in Mg-doped $LiNbO_3$ crystals to test our theory, our theoretical results for the role of $\mu$ are independent of whether $\mu$ or the effective recombination coefficient ($\gamma$) are modified in a Mg-doped crystal. Note also that the role of $\mu$ is the same as the role of the inverse recombination coefficient ($1/\gamma$) and changing either one of them by changing the photoconductivity results in the same behavior.

*Acknowledgements.* This work was supported by the U.S. Air Force Office of Scientific Research (AFOSR) and by a NSF-DAAD collaboration program.

## References

1. H. Coufal, D. Psaltis, G.T. Sincerbox: *Holographic date storage*. (Springer, Berlin 2000)
2. J.J. Amodei, D.L. Staebler: Appl. Phys. Lett. **18**, 540 (1971)
3. F. Micheron, G. Bismuth: Appl. Phys. Lett. **20**, 79 (1972)
4. D. von der Linde, A.M. Glass, K.F. Rodgers: Appl. Phys. Lett. **25**, 155 (1974)
5. R.A. Rupp, H.C. Külich, U. Schürk, E. Krätzig: Ferroelectrics **8**, 25 (1987)
6. H.C. Külich: Opt. Commun. **64**, 407 (1987)
7. K. Buse, A. Adibi, D. Psaltis: Nature **393**, 665 (1998)
8. A. Adibi, K. Buse, D. Psaltis: J. Opt. Soc. Am. B (2001), in press
9. A. Adibi, K. Buse, D. Psaltis: Opt. Lett. **25**, 539 (2000)
10. B.C. Grabmaier, W. Wersing, W. Koestler: J. Cryst. Growth **110**, 339 (1991)
11. A. Gerwens, K. Buse, E. Krätzig, N. Korneev, S. Stepanov: J. Opt. Soc. Am. B **15**, 2143 (1998)
12. Y. Furukawa, Y. Kitamura, Y. Ji, G. Montemezzani, M. Zgonik, C. Medrano, P. Gunter: Opt. Lett. **22**, 501 (1997)
13. R. Sommerfeldt, L. Holtmann, E. Krätzig, B.C. Grabmaier: Phys. Status Solidi A **106**, 89 (1988)
14. F.H. Mok, G.W. Burr, D. Psaltis: Opt. Lett. **21**, 896 (1996)
15. N.V. Kukhtarev, V.B. Markov, S.G. Odoulov, M.S. Soskin, V.L. Vinetskii: Ferroelectrics **22**, 949 (1979)
16. H. Guenther, R. Macfarlane, Y. Furukawa, K. Kitamura, R. Neurgaonkar: Appl. Opt. **37**, 7611 (1998)
17. L. Hesselink, S.S. Orlov, A. Liu, A. Akella, D. Lande, R.R. Neurgaonkar: Science **282**, 1089 (1998)
18. Y. Yang, A. Adibi, D. Psaltis: in preparation (2001)